Vol. 32 — N° 3 09 08 p. 295–310

GEOSTANDARDS and GEOANALYTICAL RESEARCH

Sodic Pyroxene and Sodic Amphibole as Potential Reference Materials for *In Situ* Lithium Isotope Determinations by SIMS

Michael A.W. **Marks** (1)*, Roberta L. **Rudnick** (2), Thomas **Ludwig** (3), Horst **Marschall** (4), Thomas **Zack** (3), Ralf **Halama** (2), William F. **McDonough** (2), Detlef **Rost** (5), Thomas **Wenzel** (1), Edward P. **Vicenzi** (5), Ivan P. **Savov** (6), Rainer **Altherr** (3) and Gregor **Markl** (1)

(1) Institut für Geowissenschaften, AB Mineralogie und Geodynamik, Eberhard-Karls-Universität, Wilhelmstraße 56, 72074 Tübingen, Germany
(2) Geochemistry Laboratory, Department of Geology, University of Maryland, College Park, MD 20742, USA
(3) Mineralogisches Institut, Ruprecht-Karls-Universität, Im Neuenheimer Feld 236, 69120 Heidelberg, Germany
(4) Department of Earth Sciences, University of Bristol, Wills Memorial Building, Queen's Road, Bristol BS8 1RJ, UK
(5) Department of Mineral Sciences, Smithsonian Institution, National Museum of Natural History, 10th St. and Constitution Ave., Washington, DC 20560-0119, USA
(6) School of Earth and Environments, Leeds University, Leeds LS2 9JT, UK
* Corresponding author. e-mail: michael.marks@uni-tuebingen.de

Two large pegmatitic crystals of sodic pyroxene (aegirine) and sodic amphibole (arfvedsonite) from the agpaitic igneous Ilímaussaq Complex, south Greenland were found to be suitable as reference materials for *in situ* Li isotope determinations. Lithium concentrations determined by SIMS and micro-drilled material analysed by MC-ICP-MS generally agreed within analytical uncertainty. The arfvedsonite crystal was homogeneous with [Li] = 639 ± 51 μg g^{-1} (2*s*, n = 69, MC-ICP-MS and SIMS results). The aegirine crystal shows strongly developed sector zoning, which is a common feature of aegirines. Using qualitative element mapping techniques (EPMA), the homogeneous core of the crystal was easily distinguished from the outermost sectors of the crystals. The core had a mean [Li] of 47.6 ± 3.6 μg g^{-1} (2*s*, n = 33) as determined by SIMS. The seven micro-drilled regions measured by solution MC-ICP-MS returned slightly lower concentrations (41-46 μg g^{-1}), but still overlap with the SIMS data within uncertainty. Based on MC-ICP-MS and SIMS analyses, the variation in δ^7Li was about 1‰ in each of the two crystals, which is smaller than that in widely used glass reference materials, making these two samples suitable to serve as reference materials. There was, however, a significant offset between the results of MC-ICP-MS and SIMS. The latter deviated from the MC-ICP-MS results by -6.0 ± 1.9‰ (2*s*) for the amphibole and by -3.9 ± 1.9‰ (2*s*) for the aegirine. This indicates the presence of a significant matrix effect in SIMS determinations of Li isotopes for amphibole and

Deux grands cristaux pegmatitiques, un pyroxène sodique (aegérine) et une amphibole sodique (arfvedsonite) provenant du complexe agpaïtique Ilímaussaq (sud du Groenland) ont été sélectionnés pour être des matériaux de référence lors d'analyses in situ des isotopes de Li. Les concentrations en lithium ont été déterminées par SIMS et par MC-ICP-MS sur du matériel prélevé par micro-forage. Les deux déterminations sont en accord aux erreurs analytiques près. Le cristal de arfvedsonite est homogène avec [Li] = 639 ± 51 μg g^{-1} (2s, n = 69, données MC-ICP-MS et SIMS). Le cristal d'aegérine présente des zonations très franches, comme il est classique dans les aegérines. En utilisant les techniques de cartographie chimique qualitative des éléments (EMPA) il a été possible de clairement distinguer le cœur du cristal, homogène, de ses bordures zonées. Le cœur a un [Li] moyen de 47.6 ± 3.6 μg g^{-1} (2s, n = 33) d'après l'analyse par SIMS. Les sept régions micro forées et analysées par MC-ICP-MS en solution présentent des concentrations légèrement inférieures (41-46 μg g^{-1}) mais qui néanmoins sont dans la même gamme, aux erreurs analytiques près, que celles déterminées par SIMS. Les données obtenues par MC-ICP-MS et SIMS montrent que la variation de δ^7Li dans chaque cristal est de 1‰, ce qui est bien inférieur à celle mesurée dans les verres de référence généralement utilisés. Ces deux échantillons sont donc très adaptés à une utilisation comme matériaux de référence. Il y a néanmoins un décalage significatif entre les données de MC-ICP-MS et les données

pyroxene relative to the basalt glasses used for calibration. Based on the MC-ICP-MS results, mean δ^7Li values of +0.7 ± 1.2‰ (2*s*, n = 10) for the arfvedsonite crystal and of -3.7 ± 1.2‰ (2*s*, n = 7) for the core of the aegirine crystal were calculated. Adopting these values, SIMS users can correct for the specific IMF (instrumental mass fractionation) of the ion probe used. We propose that these two crystals serve as reference materials for *in situ* Li isotope determinations by SIMS and pieces of these two crystals are available from the first author upon request.

Keywords: reference material, Li isotopes, aegirine, arfvedsonite, Ilímaussaq.

obtenues par SIMS, ces dernières diffèrent des premières de -6.0 ± 1.9‰ (2s) pour l'amphibole et de -3.9 ± 1.9‰ (2s) pour l'aegérine. Ceci démontre l'existence d'un effet de matrice non négligeable lors de l'analyse par SIMS des isotopes de Li dans des amphiboles et des pyroxènes, par rapport au verre basaltique utilisé pour la calibration. Les valeurs moyennes de δ^7Li de +0.7 ± 1.2‰ (2s, n = 10) pour le cristal d'arfvedsonite et de -3.7 ± 1.2‰ (2s, n = 7) pour le cœur du cristal d'aegérine ont été calculées à partir des données obtenues par MC-ICP-MS. Les utilisateurs de SIMS peuvent utiliser ces valeurs pour corriger leurs résultats du fractionnement de masse instrumental (IMF) spécifique à la sonde ionique utilisée. Nous proposons d'utiliser ces deux cristaux comme matériaux de référence lors de déterminations in situ des isotopes de Li par SIMS et des fragments de ces deux cristaux peuvent être demandés au premier auteur.

Mots-clés : matériau de référence, isotopes de Li, aegérine, arfvedsonite, Ilímaussaq.

Received 10 Dec 07 — Accepted 30 May 08

The precise and accurate isotopic determination of Li and its two stable isotopes (^{6}Li and ^{7}Li) is of great interest to many fields of science and technology, including the nuclear industry, astrophysics, biomedicines and geosciences (Tomascak 2004 and references therein). The large relative mass difference (about 17%) between ^{6}Li and ^{7}Li results in a large natural variation of Li isotopes of about 80‰ (Rudnick and Nakamura 2004). Recently, a number of studies show that the rapid solid-state diffusion of Li might produce large Li isotope fractionations on a μm-scale in geological materials (e.g., Richter *et al.* 2003, Beck *et al.* 2006, Jeffcoate *et al.* 2007, Rudnick and Ionov 2007, Parkinson *et al.* 2007). Therefore, *in situ* analytical techniques such as secondary ion mass spectrometry (SIMS) or laser ablation-inductively coupled plasma-mass spectrometry (LA-ICP-MS) are critical to study Li diffusion.

In such *in situ* techniques, the sample of interest is calibrated against a reference material with known concentration and/or isotopic composition. This approach works best if the reference material used for calibration is structurally and chemically as similar to the analysed sample as possible. However, to date, no crystalline reference materials are available and reference materials suitable for *in situ* techniques are restricted to glass reference materials of the NIST and the USGS series (Kasemann *et al.* 2005) materials, which are structurally very different from crystalline minerals. A matrix effect for Li isotope determination using SIMS has been reported by Kasemann *et al.* (2005) and Bell *et al.* (2005), Hauri *et al.* (2006), Ludwig *et al.* (2004) and Rosner *et al.* (2008) reported matrix effects and an influence of the primary beam current for H/D and B, respectively. However, the presence or absence of matrix effects in different materials for Li isotopes seems to be far from being fully understood (Jeffcoate *et al.* 2007) and opposing opinions on this topic exist. Given this and the absence of widely used crystalline reference materials for *in situ* Li isotope determinations, the availability of well-characterised, isotopically homogeneous mineral reference materials is imperative (see review of Tomascak 2004).

Despite the known disadvantages and because of the absence of alternatives, glass reference materials are still widely used and, unfortunately, little work has been done so far in order to use crystalline materials for evaluating *in situ* techniques (Chaussidon and Robert 1998, Decitre *et al.* 2002). Moreover, in cases where crystalline materials are used for calibration (e.g., Beck *et al.* 2004, Lundstrom *et al.* 2005, Williams and Hervig 2005), these are not established outside the respective laboratories, although this would be

necessary in order to enable inter-laboratory comparisons, to facilitate better comparisons between different methods and to improve the reliability of *in situ* Li isotope data in general.

In this study, we present Li concentration ([Li]) and Li isotope data (δ^7Li) for two chemically well-characterised crystals of Na-pyroxene (aegirine) and Na-amphibole (arfvedsonite) from south Greenland. These have been analysed using bulk analyses (MC-ICP-MS) and *in situ* techniques (SIMS, LA-ICP-MS) at the Universities of Maryland (USA) and Heidelberg (Germany). Our approach of combining MC-ICP-MS analysis of micro-drilled areas in coarse-grained minerals with detailed homogeneity tests by SIMS is a strategy that could be generally applied to various *in situ* isotope studies. The Na-amphibole arfvedsonite, for which the Ilímaussaq complex is the type locality, was named after Johann A. Arfvedson, who discovered the element Li in 1817 - additional motivation to establish arfvedsonite as a Li isotope reference material.

Sample material and analytical methods

We investigated one crystal each of Na-amphibole (arfvedsonite) and of Na-pyroxene (aegirine) from the agpaitic Ilímaussaq complex, south Greenland. Agpaitic rocks are peralkaline feldspathoid syenites [molar $(Na_2O + K_2O)/Al_2O_3$ ratio › 1], being characterised by the presence of complex Na-(Ti, Zr)-silicates (e.g., eudialyte, Sørensen 1997). For details on the geology, petrology and geochemistry of the Ilímaussaq complex, the reader is referred to Ferguson (1964), Larsen (1976), Sørensen (2001), Markl *et al.* (2001) and Marks *et al.* (2004, 2007). The two crystals are from the so-called marginal pegmatite, which generally consists of dm-sized crystals of microcline, nepheline, sodalite, aegirine, arfvedsonite and aenigmatite, with minor amounts of biotite, rinkite, astrophyllite, fluorite and other accessory minerals (Sørensen 2006, Müller-Lorch *et al.* 2007). Since Li generally behaves in a moderately incompatible way during igneous fractionation (Ryan and Langmuir 1987, Brenan *et al.* 1998), mafic minerals from such highly fractionated rock types have high [Li] (several tens to hundreds μg g^{-1}, Marks *et al.* 2004, 2007) compared to minerals from mantle rocks. These high concentrations encouraged us to establish these crystals as new reference materials for *in situ* Li isotope determination, since they cover the range of [Li] observed in common silicate minerals in both metamorphic and igneous crustal rocks (e.g., Tischendorf *et al.* 2001, Teng *et al.* 2006, Zack *et al.* 2003, Marschall *et al.* 2006).

The ~ 13.5 mm x 8 mm large amphibole crystal (sample ILM 160) was cut parallel to its c-axis; the ~ 15 mm x 11 mm large pyroxene crystal (sample ILM 163) was dissected perpendicular to its c-axis. In order to avoid contamination, both crystals were mounted, polished and cleaned following the procedure described in Marschall and Ludwig (2004). Figure 1 shows reflected light images of the two crystals, along with the locations of the various measurements.

The two crystals were analysed for their major and minor element composition with a JEOL 8900 electron microprobe in wavelength-dispersion mode at Universität Tübingen (Germany), using a beam current of 15 nA and an acceleration voltage of 15 kV. The counting time on the peak was 16 s for major elements (Si, Fe, Na) and 30-60 s for minor elements (Ca, K, Mn, Ti, Zr, Zn, Mg, Al, Cl, F). Background counting times were half of the peak counting times. The peak overlap between the Fe Lβ and F Kα lines was corrected for. To avoid Na migration under the electron beam, analyses were performed with a defocused beam of 10 μm diameter. Both natural and synthetic mineral phases were used as calibrators and processing of the raw data was carried out with the internal φρZ correction method of JEOL (Armstrong 1991).

Lithium, Be and B concentrations were determined by secondary ion mass spectrometry (SIMS) with a modified Cameca IMS 3f ion microprobe at Universität Heidelberg (Germany). Analyses were performed using a (mass-filtered) $^{16}O^-$ primary ion beam at 14.5 keV and 20 nA. Positive secondary ions were accelerated by applying a nominal voltage of 4.5 kV. The energy window was set to 40 eV. We applied the energy filtering technique with an offset of 75 eV at a mass resolution of $M/\Delta M \approx 1000$ (10% intensity ratio) to suppress interfering molecules and to minimise matrix effects (Ottolini *et al.* 1993). Secondary ion intensities of ^{7}Li, ^{9}Be and ^{11}B were normalised to the count rate of ^{30}Si and calibrated against the NIST SRM 610 glass reference material using the concentrations reported in Pearce *et al.* (1997). A 5 min pre-sputtering time was implemented on each spot. Employing a 750 μm field aperture limited the imaged field to a diameter of ~ 12 μm so that only secondary ions originating from the centre of the sputtered crater contributed to the analyses. This technique reduced the influence of surface contamination to an apparent B concentration below the detection limit of ~ 2 ng g^{-1} B (Marschall and Ludwig 2004). Since the mass spectrometer's and the counting system's background was only 0.02 ±

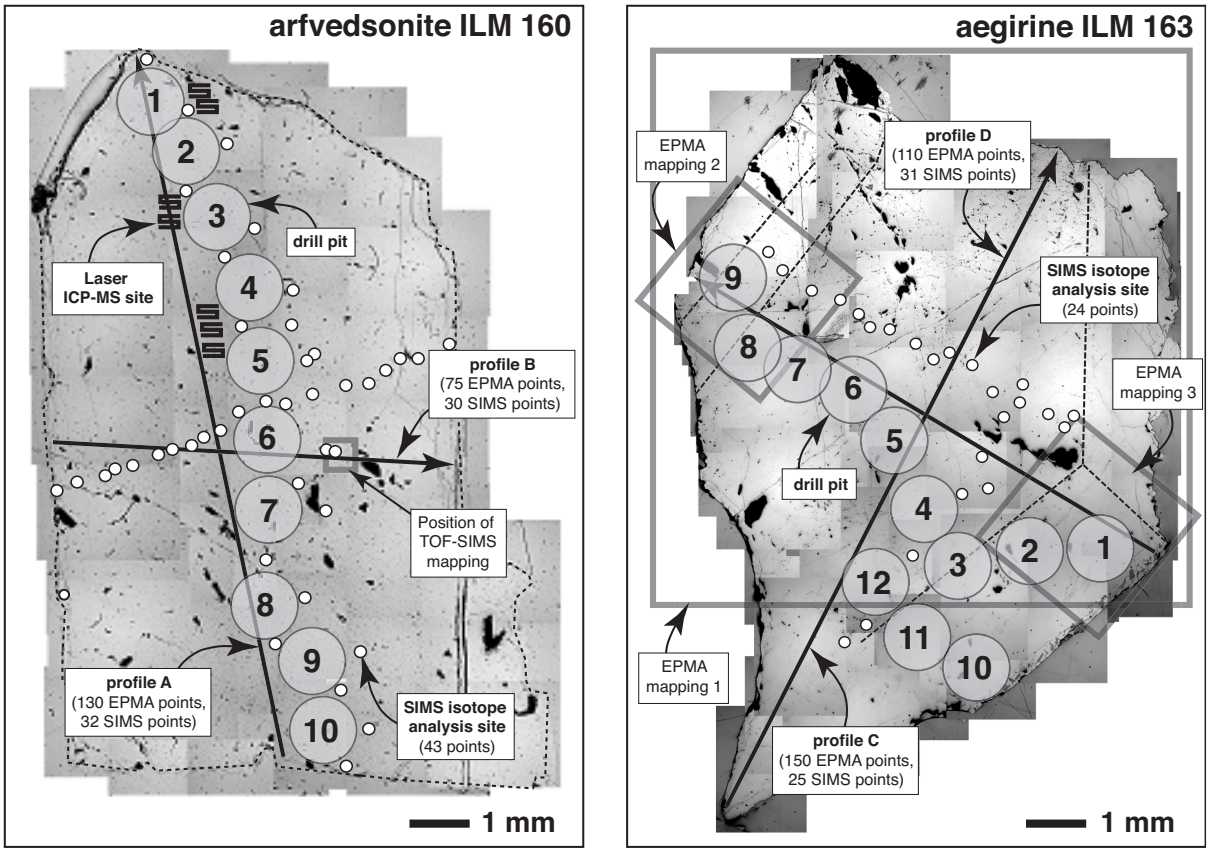

Figure 1. Reflected light images of the two crystals investigated in this study along with the locations of the various measurements performed. The dashed lines in the aegirine picture represent the borders of the different crystallographic sectors, based on EPMA mapping (see Figures 5 and 6).

0.01 s^{-1}, corresponding to concentrations of ≤ 1 ng g^{-1}, no further correction was necessary.

Imaging time-of-flight secondary ion mass spectrometry (ToF-SIMS) was used to map qualitatively the distribution of Li, Be, B and other elements. Measurements were acquired with the ToF-SIMS IV instrument from ION-TOF GmbH at the Smithsonian Institution, Washington (USA). The 500 μm x 500 μm secondary ion images were obtained using a 25 kV Ga^+ primary ion beam in the so-called "high current bunched mode" that offers high secondary ion count rates, the best mass resolution (M/ΔM ~ 8000 for Si, full width half maximum) and a lateral resolution of ~ 5 μm.

The Li isotopic compositions of the two crystals were investigated by three independent methods:

(i) Powders derived from micro-drilling were analysed by solution MC-ICP-MS at the University of Maryland (USA). The diameter of the diamond drills was 1 mm and the amount of powder retrieved varied between 1 and 4 mg. Full details of the method of Li isotope determinations used here are provided in Rudnick *et al.* (2004) and Teng *et al.* (2004). Monitoring the Li yield from column chemistry is important in evaluating the quality of the Li isotope data (Chan *et al.* 2002). Marks *et al.* (2007) show that a › 96% Li yield is sufficient to obtain accurate δ^7Li values. In order to monitor the Li yield from chromatographic separation after peak elution, cuts (2 ml each) were analysed for their [Li] using a ThermoFinnigan Element2, single collector ICP-MS (see below). As can be seen in Table 3, the Li yield during column separation was ≥ 96% in all samples and no correlation between Li yield and [Li] or δ^7Li value was observed demonstrating the reliability of the data.

The total Li procedural blank during this study was ~ 50 pg Li with a δ^7Li value of -45‰, which accounts for both procedural and instrumental blank. This blank is negligible compared to the amount of Li processed for the samples (generally › 50 ng), and the long-term precision of ± 1‰ (2*s*). Thus, no blank correction was

necessary. All Li isotope results are reported in the δ^7Li notation with δ^7Li = 1000 x [(^{7}Li/^{6}Li$_{sample}$)/(^{7}Li/^{6}Li$_{RM}$)-1] relative to the L-SVEC reference material (Flesch *et al.* 1973) and are calculated by comparison of the unknown sample to the average of two bracketing L-SVEC analyses, as described in Tomascak *et al.* (1999). For two blocks of twenty ratios each, the in-run precision of ^{7}Li/^{6}Li measurements was generally within ± 0.2‰, with no systematic change in the ^{7}Li/^{6}Li ratio. The external precision, based on repeat runs of Li standard solutions, was within ± 1‰ (2*s*) or better. During the course of this study reference materials UMD-1 and IRMM-016 gave δ^7Li values of +54.5 ± 0.5‰ (2*s*, n = 26) and -0.8 ± 0.4‰ (2*s*, n = 14), respectively, values falling in the previously established ranges (e.g., Teng *et al*. 2006). Lithium concentrations of the samples were determined by voltage comparisons obtained for the sample with that of the two bracketing L-SVEC reference materials of known concentration, and then adjusting for the sample mass. The precision and accuracy of this method is better than 10% based on comparison with isotope dilution analyses (Teng *et al.* 2004).

(ii) SIMS Li isotope determinations were performed with the modified Cameca IMS 3f ion microprobe at Universität Heidelberg. Modifications to this machine included new, fast electronics for the mass spectrometer's magnet (active compensation of the magnet's eddy current fields for rapid field stabilisation) and a counting system for the electron multiplier with a dead time of ~ 18 ns. A 14.5 keV $^{16}O^-$ (mass-filtered) primary ion beam with a current of I_P = 10 nA and a spot size of ~ 25 μm were used. Secondary ions were accelerated to 4.5 keV, the energy window was set to 100 eV and no offset was applied. N = 100 cycles were measured on each analysis spot with integration times of 3.518 s and 1.003 s on ^{6}Li and ^{7}Li, respectively. For each cycle, the ^{6}Li signal was integrated for 1.759 s before and after collection of the ^{7}Li signal, thus minimising the influence of increasing or decreasing count rates (which were corrected for the counting system's dead time of 18 ns) on the measured isotope ratio. Pre-sputtering lasted for 5 min (including automatic mass calibration of the ^{6}Li and the ^{7}Li peaks) and the settling time between two masses was 200 ms, resulting in a total analysis time of approximately 14 min. Instrumental mass fractionation α_{inst} was determined by using synthetic basaltic glasses GSD-1G and GSE-1G as reference materials. δ^7Li values for these glasses were taken from Kasemann *et al.* (2005): δ^7Li (GSD-1G) = +31.42‰ and δ^7Li (GSE-1G) = +31.31‰ (mean value of MC-ICP-MS and TIMS analyses).

In order to obtain similar count rates *i* (Li) on both reference samples (GSD-1G: 39 μg g^{-1} Li, GSE-1G: 380 μg g^{-1} Li, Jochum *et al.* 2005) and both samples (ILM160: ~ 650 μg g^{-1}, ILM163: ~ 46 μg g^{-1}) the width of the mass spectrometer's entrance slit was reduced for GSE-1G and ILM160. The mass resolution was always sufficiently high to suppress any significant contribution of the ^{6}LiH peak at the centre of the ^{7}Li peak (we report our mass resolution M/ΔM at 0.01% intensity ratio). Ten analyses on the reference sample were performed before analysing the unknown sample and ten analyses thereafter. The mean α_{inst} and its relative standard deviation RSD of these twenty analyses are reported here. For ILM160 (*i* (^{7}Li) ≈ 2.1 x 10^5 s^{-1}) GSE-1G was used as reference: α_{inst} = 1.0215, RSD (α_{inst}) = 0.5‰, M/ΔM = 742 and *i* (^{7}Li) ≈ 1.2 x 10^5 s^{-1}. For ILM163 (*i* (^{7}Li) ≈ 2.6 x 10^5 s^{-1}) GSD-1G was used: α_{inst} = 1.0197, RSD (α_{inst}) = 0.8‰, M/ΔM = 592 and *i* (^{7}Li) ≈ 1.6 x 10^5 s^{-1}. The in-run precision of a single analysis on the samples is reported as the standard deviation of the mean δ^7Li value $s_{mean} = s\sqrt{N}$. The average s_{mean} for the reference samples was 0.7‰ on GSE-1G and 0.6‰ on GSD-1G and was dominated by counting statistics.

The goal of the SIMS Li isotope determinations was to have exactly (*N*, I_P, total time) or nearly ([Li], *i* (Li)) the same conditions for the unknown and the reference samples in order to preclude an effect of these parameters on the result. It is remarkable that closing the entrance slit of the mass spectrometer changed α_{inst} only by +1.8‰ while reducing the count rate by a factor of ~ 10.

(iii) *In situ* Li isotopic determinations on the amphibole (ILM 160) were also obtained by LA-ICP-MS at the University of Maryland (USA). Here, a New Wave UP-213 laser was coupled to a ThermoFinnigan Element2 ICP mass spectrometer. A 40 μm spot was used with a repetition rate of 8 Hz. Output power was 45%, corresponding to ~ 3 J cm^{-2}. Measurements were made in rastering mode with a scan speed of 10 μm s^{-1}. One analysis comprised 5000 runs, and the dwell times during each cycle for ^{6}Li and ^{7}Li were 20 and 5 ms, respectively, separated by a settling time of 1 ms between the peaks. While the counting precision for individual measurements was ≤ 0.7‰, the 2*s* uncertainty of the mean ^{7}Li/^{6}Li ratio was ± 5‰. This large uncertainty is obviously not an effect of limited counting statistics. We suspect that variations in the mean atomic weight within the analysed material, but also drift introduced by the ICP source to the system are the

predominate reasons for this uncertainty. When the plasma passes through the sample and skimmer cones, the population of ions changes dramatically. First, the electrical potentials of these cones are such that the electrons in the plasma are removed via conduction along the cone surface. Second, as the ion beam passes through the cones, it is significantly affected by space-charge forces, which cause it to expand, with the lighter ions (i.e., Li) being more affected than heavy ions (i.e., U). The Li isotope results from LA-ICP-MS analyses (-2.2 to +1.6‰, n = 7) overlapped with MC-ICP-MS and SIMS data (see below) when standardised relative to NIST SRM 610 glass [a value of +31.3 ± 0.5‰ (2*s*, n = 3) was determined by MC-ICP-MS solution analysis, which is in agreement with that reported by Kasemann *et al.* (2005)]. However, because of the large uncertainty, these analyses are not discussed further.

Results and discussion

Amphibole ILM 160

Major, minor and trace element composition: Following the nomenclature of Leake *et al.* (1997), the amphibole belongs to the sodic group and is an arfvedsonite, with a uniform high X_{Fe} value ($Fe^{2+}/(Fe^{2+} + Mg^{2+})$) of 0.99. Its composition (Figure 2, Table 1) is characterised by high concentrations of FeO_{total} (34.85 ± 1.83% m/m) and Na_2O (7.65 ± 0.46% m/m) and low concentrations of Al_2O_3 (1.92 ± 0.12% m/m), K_2O (1.87 ± 0.09% m/m) and CaO (1.49 ± 0.08% m/m). Minor elements determined include MnO (0.62 ± 0.04% m/m), TiO_2 (0.54 ± 0.03% m/m), ZrO_2 (0.28 ± 0.04% m/m), ZnO (0.09 ± 0.05% m/m) and MgO (0.15 ± 0.03% m/m). The mean F content was 0.82 ± 0.10% m/m, whereas Cl was generally below the EPMA detection limit (200 μg g^{-1}, n = 205). Aluminium showed a slight enrichment in the innermost core of the crystal, while all other elements showed no systematic core to rim variation (Figure 2 upper left). These data are in accordance with previously published data on Ilímaussaq amphiboles (Marks *et al.* 2004, Krumrei *et al.* 2006, Müller-Lorch *et al.* 2007) and with the expected highly evolved character of pegmatitic amphiboles in peralkaline igneous rocks.

Beryllium and B concentrations were homogeneous and had mean values of 3.75 ± 0.22 μg g^{-1} (2*s*, n = 62) and 1.20 ± 0.08 μg g^{-1} (2*s*, n = 62), respectively (Figure 2). Beryllium was enriched in one spot that was adjacent to a fracture, having a concentration of ~ 5.1 μg g^{-1}. Interestingly, Be was only enriched in one out of the three spots, where Li was significantly enriched (see below).

Li concentrations: The Li concentrations of the arfvedsonite determined by SIMS varied between 601 and 672 μg g^{-1} in profile A (n = 32, Figure 2, lower left) and between 594 and 766 μg g^{-1} in profile B (n = 30, Figure 2, lower right) and showed no systematic zoning. Three out of the thirty data points in profile B showed significantly higher Li concentrations (747-766 μg g^{-1}) compared to all other SIMS data points (594-672 μg g^{-1}, n = 59), which gave an average of 634 ± 20 μg g^{-1}. These three data points lay close to a fracture zone in the crystal. ToF-SIMS imaging verified the local enrichment of Li and several other trace elements such as Be, Rb, K, Zn, but not for B (Figure 3). We thus consider this Li enrichment to be a secondary feature and we excluded these three data points from the calculation of averages. The Li concentrations determined from the drilled samples varied between 628 and 715 μg g^{-1} (mean of 667 ± 35 μg g^{-1}, n = 10) and compared well with the SIMS results. Excluding the three data points adjacent to the fracture zone from profile B, the calculated mean Li concentration from the two profiles and the drilled samples was then 639 ± 51 μg g^{-1} (2*s*, n = 69), which we consider to be the best estimate of Li concentration for this specimen.

Li isotopic composition: The micro-drilled MC-ICP-MS profile (n = 10) revealed homogeneous δ^7Li values between -0.2 and +1.9‰, with an average value of +0.7 ± 1.2‰ (2*s*, Figure 4, Table 3). The Li isotope data obtained by SIMS (n = 43) showed a similar homogeneous Li isotopic composition, but measured δ^7Li values had a mean of -5.3 ± 1.1‰ (2*s*, Figure 4), which is a systematic deviation of -6.0 ± 1.9‰ (2*s*) from the MC-ICP-MS data.

Pyroxene ILM 163

Major, minor and trace element composition: This aegirine crystal showed spectacular sector zoning, similar to aegirines from the Ilímaussaq complex previously described by Larsen (1981) and Shearer and Larsen (1994). The core [001] was enriched in Ca, Fe^{2+} and Zr, whereas the prism sectors {110}, {100} and {010} were enriched in Na, Fe^{3+}, Al and Ti (Table 2, Figures 5 and 6). Following the nomenclature of Morimoto (1989), both the relatively Ca-rich core and the Na-rich outer sectors of the crystal have aegirine

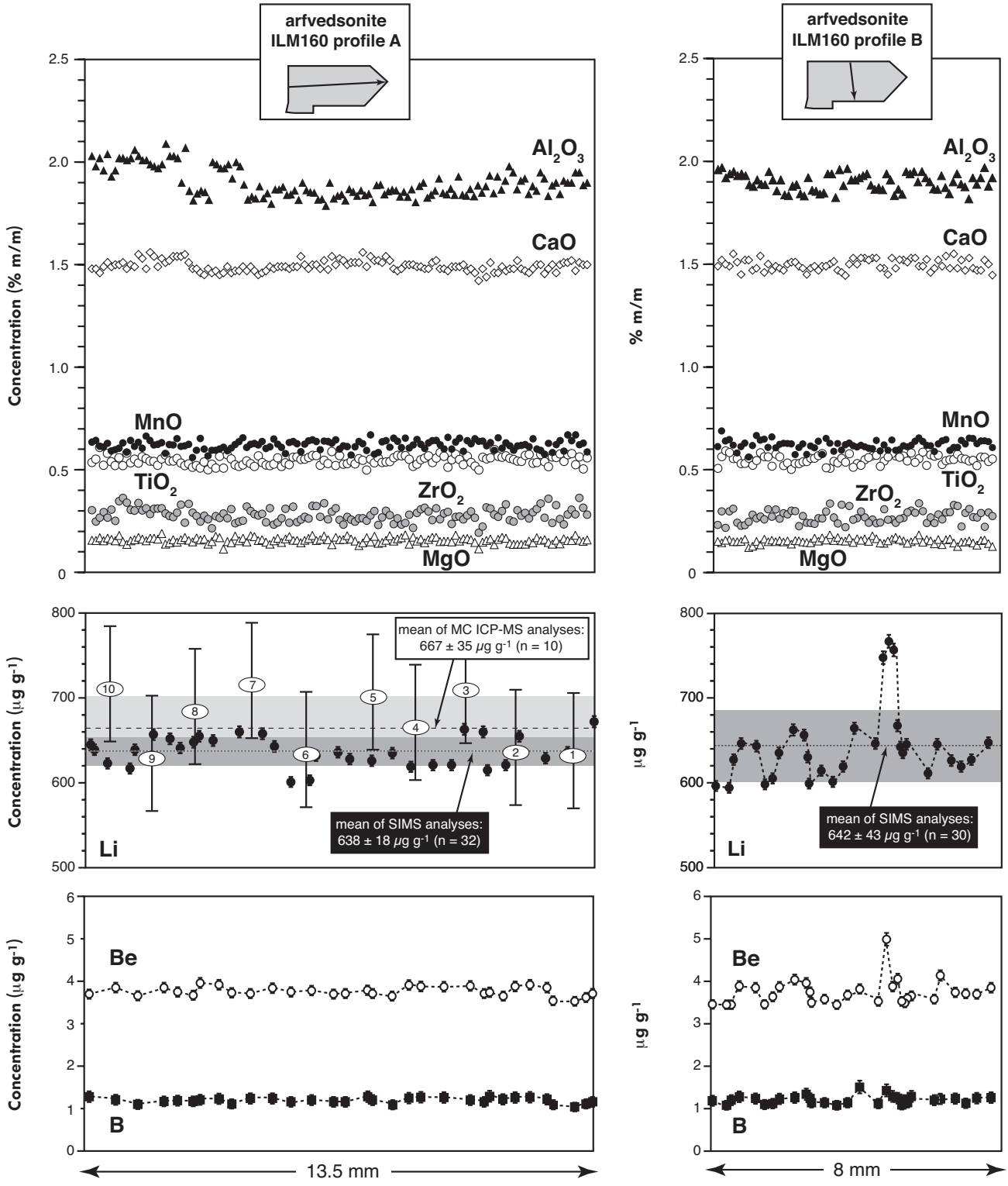

Figure 2. Results from two measurement profiles (A and B) through the arfvedsonite crystal ILM 160. The upper two diagrams show electron probe microanalysis data for selected elements, the middle diagrams present Li concentrations (MC ICP-MS and SIMS analyses) and the lower diagrams show Be and B contents (SIMS). The error bars for Li, Be and B concentrations determined by SIMS represent the 2*s* uncertainty. The white ellipses in the middle left diagram represent the MC ICP-MS results for the ten drill pits, whereas the numbers correspond to those given in Figure 1 and Table 3.

Table 1.
Representative electron probe microanalyses of arfvedsonite ILM 160 together with the calculated mean composition of the homogeneous core region

						Mean composition	Standard deviation (n = 205, 1*s*)
% m/m							
SiO_2	47.59	47.89	47.98	48.11	48.17	47.95	± 0.85
TiO_2	0.51	0.49	0.53	0.53	0.50	0.54	± 0.03
Al_2O_3	1.94	1.91	1.86	2.00	2.01	1.92	± 0.12
ZnO	0.08	0.06	0.13	0.08	0.09	0.09	± 0.05
Li_2O*	0.14	0.14	0.14	0.14	0.14	0.14	± 0.01
FeO	34.73	34.95	35.04	35.17	34.52	34.85	± 1.83
MnO	0.62	0.62	0.60	0.62	0.58	0.62	± 0.04
MgO	0.15	0.14	0.16	0.18	0.15	0.15	± 0.03
CaO	1.46	1.50	1.54	1.46	1.51	1.49	± 0.08
Na_2O	7.58	7.48	7.60	7.74	7.48	7.65	± 0.46
K_2O	1.88	1.95	1.95	1.83	1.93	1.87	± 0.09
ZrO_2	0.29	0.29	0.33	0.25	0.31	0.28	± 0.04
Cl	0.01	0.01	0.00	0.00	0.00	0.00	-
F	0.83	0.82	0.82	0.80	0.81	0.82	± 0.10
Total	97.68	98.25	98.70	98.93	98.22	98.36	-
Formulae based on 16 cations and 23 oxygens							
Si	7.65	7.67	7.64	7.63	7.71	7.66	
Al	0.39	0.38	0.37	0.39	0.40	0.38	
Ti	0.06	0.06	0.06	0.06	0.06	0.06	
Zn	0.01	0.01	0.02	0.01	0.01	0.01	
Li	0.08	0.08	0.09	0.09	0.09	0.09	
Fe^{3+}	0.98	0.92	1.00	1.01	0.82	0.97	
Mg	0.04	0.03	0.04	0.04	0.04	0.04	
Fe^{2+}	3.69	3.76	3.67	3.66	3.80	3.68	
Mn	0.08	0.08	0.08	0.08	0.08	0.08	
Ca	0.25	0.26	0.26	0.25	0.26	0.25	
Na	2.36	2.32	2.35	2.38	2.32	2.37	
K	0.39	0.40	0.40	0.37	0.39	0.38	
Zr	0.02	0.02	0.03	0.02	0.02	0.02	
Cl	0.00	0.01	0.00	0.01	0.01	0.00	
F	0.42	0.42	0.41	0.40	0.41	0.41	
Sum	16.00	16.00	16.00	16.00	16.00	16.00	

* Li concentrations are given after the SIMS results.

composition. The chemical changes from the outermost part of the crystal towards the border with the core were gradual and were followed by a distinct compositional step at the sector boundaries (Figure 6). In contrast, the core was homogeneous (FeO_{total} = 28.95 ± 0.35% m/m, Na_2O = 11.30 ± 0.21% m/m, CaO = 4.30 ± 0.33% m/m, Al_2O_3 = 0.70 ± 0.03% m/m, ZrO_2 = 0.64 ± 0.05% m/m, TiO_2 = 0.41 ± 0.04, MnO = 0.27 ± 0.03% m/m, ZnO = 0.04 ± 0.03% m/m and MgO = 0.02 ± 0.01% m/m, n = 165).

Beryllium and B concentrations varied systematically as well. Compared to the homogeneous core, which contained 0.88 ± 0.04 μg g^{-1} Be (n = 33) and 0.23 ± 0.03 μg g^{-1} B (n = 33), Be was slightly depleted (~ 0.71 μg g^{-1}) and B was slightly enriched (~ 0.33 μg g^{-1}) in the outer sectors of the crystal (Figure 6).

Li concentrations: As for the major and minor elements, [Li] determined by SIMS varied systematically, with relatively high concentrations (70-75 μg g^{-1}) in the outer sectors and 47.6 ± 3.6 μg g^{-1} (2*s*, n = 33) in the homogeneous core (Figure 6). Within the outer prism sectors [Li] was either constant (Profile C) or showed a gradual decrease towards the core, or even more complicated profiles (Profile D). The twelve micro-drilled samples revealed the same systematic pattern. Data for the core varied between 41 and 46 μg g^{-1} (n = 7) and between 54 and 56 μg g^{-1} for the prism sectors (n = 5; Table 3, Figure 6) and overlapped within uncertainty with the SIMS data.

Li isotopic composition: The micro-drill MC-ICP-MS data revealed a δ^7Li of -4.8 ± 0.4‰ (n = 5) for the rim and -3.7 ± 1.2‰ (n = 7) for the core of the crystal

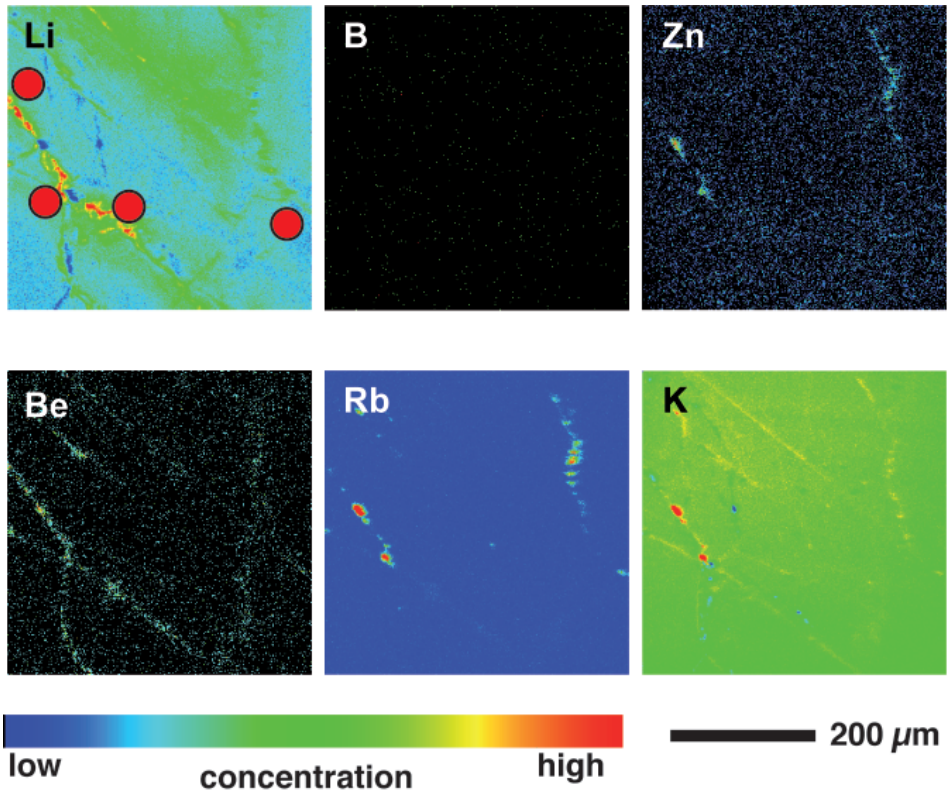

Figure 3. ToF-SIMS secondary ion distribution images of selected elements, showing increased concentrations along small cracks (the approximate position of this mapping of arfvedsonite sample ILM160 is indicated in Figure 1). Lithium, Be, Rb, Zn and other elements (which are not shown here) were enriched along the cracks, K was depleted and the B content was not significantly influenced in these areas (see also Figure 2, lower right). The four red dots in the Li-map are SIMS pits, with the three on the left corresponding to the data points with high Li concentrations (compare with Figure 2).

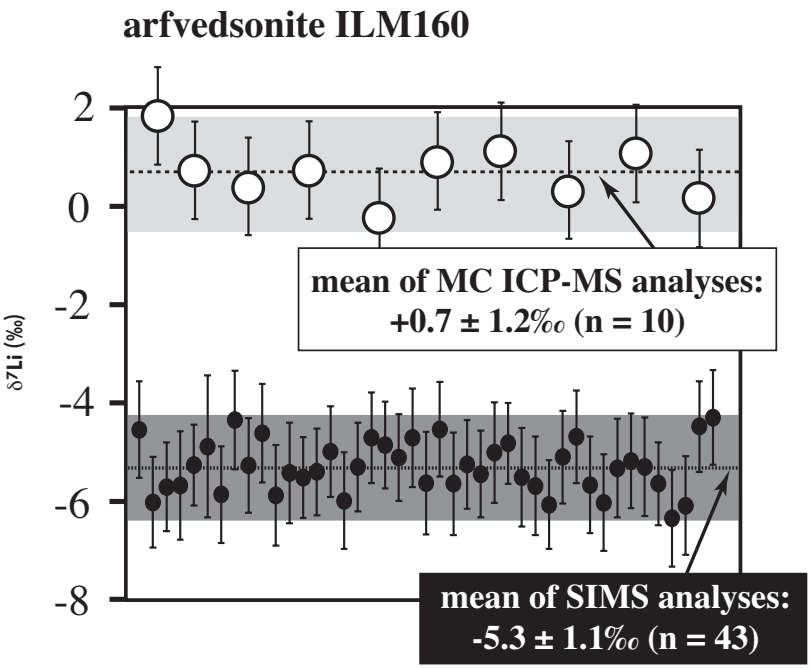

Figure 4. Lithium isotopic composition of the arfvedsonite (ILM 160) as determined by SIMS (n = 43) and MC ICP-MS (n = 10).

Table 2.
Representative electron probe microanalyses of aegirine ILM 163 together with the calculated mean composition of the homogeneous core region

	Rim	Rim	Rim	Rim	Core	Core	Core	Mean composition of core region	Standard deviation (n = 165, 1*s*)
% m/m									
SiO_2	51.20	51.04	50.09	49.88	49.83	49.98	49.51	49.85	± 0.65
TiO_2	0.68	0.77	0.40	0.40	0.40	0.42	0.42	0.41	± 0.04
Al_2O_3	0.98	1.01	0.60	0.78	0.67	0.73	0.67	0.70	± 0.03
FeO (total)	28.25	28.86	29.03	29.05	28.93	28.88	29.18	28.95	± 0.35
MnO	0.24	0.20	0.28	0.27	0.26	0.27	0.28	0.27	± 0.03
ZnO	0.05	0.04	0.03	0.05	0.02	0.09	0.09	0.04	± 0.03
MgO	0.04	0.03	0.03	0.03	0.03	0.03	0.04	0.02	± 0.01
CaO	3.16	3.11	4.96	4.36	4.41	4.33	4.37	4.30	± 0.33
Na_2O	11.88	12.05	10.87	11.11	11.13	11.19	11.09	11.30	± 0.21
ZrO_2	0.27	0.29	0.62	0.65	0.67	0.69	0.64	0.64	± 0.05
Total	96.76	97.39	96.90	96.47	96.36	96.57	96.29	96.48	
Ferric Total	99.63	100.40	99.75	99.38	99.28	99.45	99.37	99.47	
Formulae based on 4 cations and 6 oxygens									
Si	1.98	1.96	1.96	1.95	1.95	1.96	1.95	1.95	
Al	0.04	0.05	0.03	0.04	0.03	0.04	0.04	0.03	
Fe^{3+}	0.83	0.87	0.83	0.86	0.86	0.85	0.87	0.88	
Ti	0.02	0.02	0.01	0.01	0.01	0.01	0.01	0.01	
Zr	0.01	0.01	0.01	0.01	0.01	0.01	0.01	0.01	
Zn	0.00	0.00	0.00	0.00	0.00	0.00	0.00	0.00	
Mg	0.00	0.00	0.00	0.00	0.00	0.00	0.00	0.00	
Fe^{2+}	0.08	0.06	0.11	0.10	0.09	0.06	0.07	0.07	
Mn	0.01	0.01	0.01	0.01	0.01	0.01	0.01	0.01	
Ca	0.13	0.13	0.21	0.18	0.19	0.17	0.18	0.18	
Na	0.89	0.90	0.82	0.84	0.85	0.85	0.86	0.86	
Sum	4.00	4.00	4.00	4.00	4.00	4.00	4.00	4.00	

Table 3.
Lithium isotopic data (MC-ICP-MS), Li yield from column chemistry and Li concentration (MC-ICP-MS) for micro-drilled arfvedsonite (ILM160) and aegirine (ILM163)

Drill site	Sample mass (mg)	δ^7Li (‰)	Li yield (%)	Li concentration ($\mu g\ g^{-1}$)
Arfvedsonite ILM 160				
1	0.98	-0.2	99.2	628
2	0.93	0.4	98.9	632
3	1.30	0.7	99.6	708
4	2.53	0.7	99.3	651
5	2.71	0.9	99.3	701
6	1.85	1.1	98.7	631
7	1.92	0.3	99.6	715
8	1.29	1.9	98.0	671
9	1.98	1.1	96.1	629
10	2.08	0.2	99.1	705
Aegirine ILM 163				
1	2.86	-4.9	99.1	55
2	2.82	-4.7	99.4	54
3	2.37	-3.7	99.0	46
4	0.96	-4.4	99.0	41
5	3.00	-3.3	98.4	43
6	2.52	-3.2	98.8	42
7	2.49	-4.6	98.5	44
8	3.58	-3.1	97.2	45
9	2.86	-4.5	99.4	56
10	2.97	-5.0	98.7	55
11	1.70	-4.9	98.8	55
12	1.89	-3.9	98.6	43

Figure 5. Three EPMA maps of aegirine crystal ILM 163. The positions of the maps are indicated in Figure 1. The inner sector is enriched in Ca (and Zr, not shown here) whereas the outer prism sectors are enriched in Ti (and Na and Al, both not shown here).

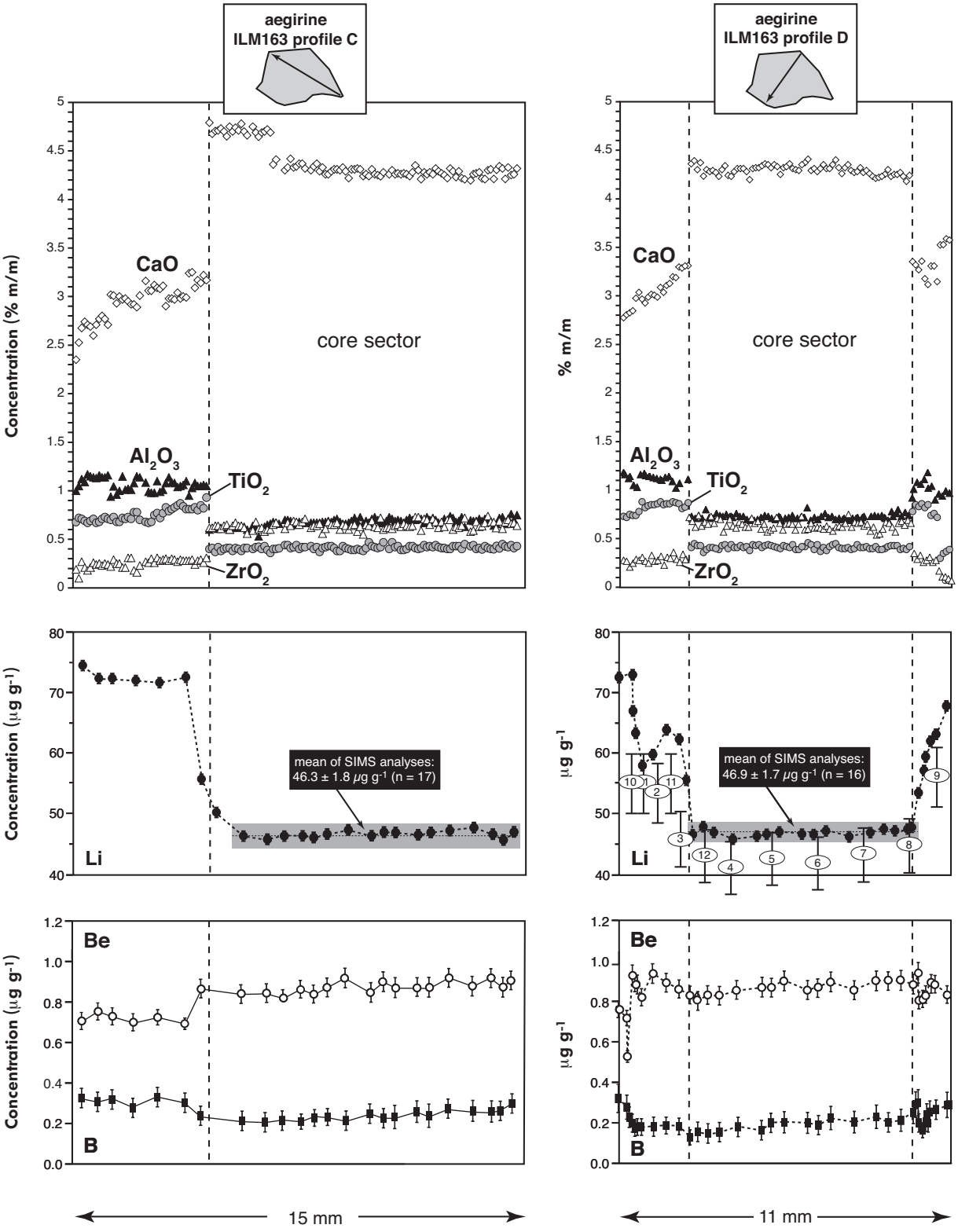

Figure 6. Two measurement profiles (C and D) through the aegirine crystal ILM 163. The upper two diagrams show electron probe microanalysis data for selected elements, the middle diagrams present Li concentrations (MC ICP-MS analyses and SIMS analyses) and the lower diagrams show Be and B contents (SIMS). The error bars for Li, Be and B concentrations determined by SIMS represent the 2*s* uncertainty. The white ellipses in the middle right diagram represent the MC ICP-MS results for the ten drill pits, whereas the numbers correspond to those given in Figure 1 and Table 3.

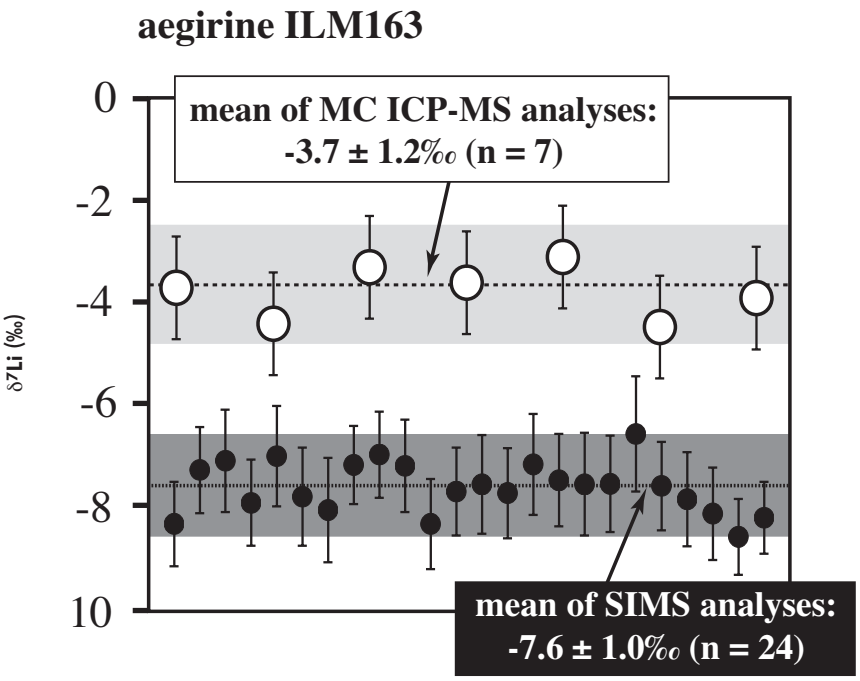

Figure 7. Lithium isotopic composition of the core of the aegirine crystal (ILM 163) as determined by SIMS (n = 24) and MC-ICP-MS (n = 7).

(Figure 7). Despite the overlap between these mean values, we focus in the following on the core of the crystal. The mean of the twenty-four SIMS analyses performed in the core of the crystal was -7.6 ± 1.0‰. Again, this is a significant offset from the MC-ICP-MS data, and again the SIMS data were isotopically lighter than the MC-ICP-MS data. The deviation from the latter was in this case 3.9 ± 1.9‰ (2*s*).

Presence of a matrix effect in SIMS Li isotope determination

Based on the SIMS analytical conditions - which were tailored to be as similar as possible for the unknown and the reference samples - we found a significant deviation of the SIMS results from MC-ICP-MS measurements. For both crystals, SIMS δ^7Li values were consistently lower than the MC-ICP-MS values. In our case this difference was -6.0 ± 1.9‰ (2*s*) for the amphibole and -3.9 ± 1.9‰ (2*s*) for the pyroxene, respectively. An even larger deviation (~ -10‰) was reported for NIST SRM 610, 612 and 614 glasses by Kasemann *et al.* (2005). Bell *et al.* (2007) report a significant change of α_{inst} when analysing olivines with compositions between Fo74 and Fo94.

In the light of these and of our results it becomes clear that SIMS Li isotope determination requires more than only one well defined reference material such as the USGS glasses in order to ascertain accurate results when analysing a variety of minerals. The two crystals introduced and analysed in this work may be used to check accuracy for similar pyroxenes and amphiboles, but this can only be a first step. In order to confirm or establish the accuracy of SIMS Li isotope determinations in general, structurally different minerals as well as other pyroxenes and amphiboles with different chemical composition (e.g., different X_{Mg}) will be needed.

Summary

Lithium concentrations and δ^7Li values for two natural crystals, one aegirine and one arfvedsonite, were determined by SIMS and micro-drill MC-ICP-MS. Both crystals have large homogeneous areas on a mm-scale, which are comparable in homogeneity to artificial glass reference materials. However, some care has to be taken to avoid chemical heterogeneities (e.g., cracks and sector zones), which can easily be identified by element microprobe imaging techniques. These two crystals thus appear to be suitable reference materials for *in situ* Li isotope determinations by SIMS.

Their Li concentrations differ by about one order of magnitude and, taken together, cover a significant portion of the range observed in common silicate minerals in crustal rocks. For example, Li concentrations for pyroxenes and amphiboles from high-pressure metamorphic rocks generally vary between several tens to hundreds of μg g^{-1} (e.g., Zack *et al.* 2003, Marschall *et al.* 2006) and Li concentrations for micas from igneous and metamorphic rocks are one to two orders

of magnitude higher (e.g., Tischendorf *et al.* 2001, Teng *et al.* 2006).

Structurally, they represent important and common silicates for both mantle and crustal rocks and are thus a significant improvement over glass reference materials. Compared to mantle minerals and minerals from primitive magmatic rocks, their Li content is about one to two orders of magnitude higher (e.g., Seitz *et al.* 2004, Ottolini *et al.* 2004, Rudnick and Ionov 2007, Halama *et al.* 2007). This does, however, not preclude their use as reference materials for *in situ* Li isotope work, since both minerals can be analysed with one of the USGS glasses as reference in order to check for possible matrix effects and because high concentrations and count rates are not a problem *per se*. Of course, publicly available homogeneous mantle minerals with typical mantle Li concentrations would be very useful reference materials as well.

The two crystals are isotopically homogeneous within the precision of the applied methods. There was, however, a significant deviation of SIMS data from MC-ICP-MS data (-6.0 ± 1.9‰ (2*s*) for ILM160 and -3.9 ± 1.9‰ (2*s*) for ILM163), which indicates the presence of a matrix effect for amphibole and pyroxene (relative to the basalt glasses used for calibration) in SIMS analysis for Li isotopes. No matter whether this is a "real" matrix effect or another hitherto unidentified analytical problem - the necessity of minerals as reference materials to ensure the accuracy of δ^7Li SIMS analysis is obvious.

These crystals are the first natural samples of sufficient quantity that have been satisfactorily characterised for this purpose. Some of the so far investigated RM glasses show extensive variations in both their Li concentration and isotope composition (e.g., glass BIR-1G; Kasemann *et al.* 2005). The variation in δ^7Li of about 1‰ in the crystals of this study is of the same order or even better than that in widely used glass reference materials (e.g., GS, BCR and NIST glasses; Kasemann *et al.* 2005).

Pieces of these two crystals can be obtained from the first author upon request. From the amphibole crystal and from the pyroxene core region we hold each around 5 g, enough material to supply SIMS laboratories willing to determine Li isotopes routinely. Splits of these crystals are available to colleagues using SIMS who are, in return, invited to contribute to the SIMS values of this pyroxene and amphibole to further examine their coherence and to establish these two crystals as widely-used reference materials. This will facilitate inter-laboratory comparisons and improve the reliability of *in situ* Li isotope data in general.

Acknowledgements

Financial support for this work was granted by the Deutsche Forschungsgemeinschaft (grant Ma2563/2-1) and NSF grants EAR0208012 and EAR0609689. Fang-Zhen Teng, Igor Puchtel, Jeffrey Ryan and Richard Ash are thanked for valuable help during the analytical work in College Park, Maryland. The constructive comments of two anonymous reviewers and the editorial handling of Mireille Polvé are acknowledged. This is Contribution to the Mineralogy of Ilímaussaq No. 135.

References

Armstrong J.T. (1991)
Quantitative elemental analysis of individual microparticles with electron beam instruments. In: Heinrich K.F.J. and Newbury D.E. (eds), Electron Probe Quantitation. Plenum Press (New York and London), 261-315.

Beck P., Chaussidon M., Barrat J.A., Gillet P. and Bohn M. (2006)
Diffusion induced Li isotopic fractionation during the cooling of magmatic rocks: The case of pyroxene phenocrysts from nakhlite meteorites. Geochimica et Cosmochimica Acta, 70, 4813-4825.

Beck P., Barrat J.A., Chaussidon M., Gillet P. and Bohn M. (2004)
Li isotopic variations in single pyroxenes from the Northwest Africa 480 shergottite (NWA 480): A record of degassing of Martian magmas? Geochimica et Cosmochimica Acta, 68, 2925-2933.

Bell D., Hervig R.L. and Buseck P.R. (2007)
Li isotope studies of mantle-derived olivine by SIMS. Geochimica et Cosmochimica Acta, 71, 15S, A75.

Bell D.R., Hervig R.L. and Buseck P.R. (2005)
Li-isotope studies of olivine in mantle xenoliths by SIMS. Lunar and Planetary Science Abstracts XXXVI, 2178.

Brenan J.M., Neroda E., Lundstrom C.C., Shaw H.F., Ryerson F.J. and Phinney D.L. (1998)
Behaviour of boron, beryllium, and lithium during melting and crystallization: Constraints from mineral-melt partitioning experiments. Geochimica et Cosmochimica Acta, 62, 2129-2141.

Chan L.H., Leeman W.P. and You C.-F. (2002)
Lithium isotopic composition of Central American Volcanic Arc lavas: Implications for modification of sub-arc mantle by slab-derived fluids: Corrections. Chemical Geology, 182, 293-300.

references

Chaussidon M. and Robert F. (1998)
$^{7}Li/^{6}Li$ and $^{11}B/^{10}B$ variations in chondrules from the Semarkona unequilibrated chondrite. Earth and Planetary Science Letters, 164, 577-589.

Decitre S., Deloule E., Reisberg L., James R.H., Agrinier P. and Mével C. (2002)
Behavior of Li and its isotopes during serpentinization of oceanic peridotites. Geochemistry Geophysics Geosystems 3, 1007, doi:10.1029/2001GC000178,2002.

Ferguson J. (1964)
Geology of the Ilimaussaq alkaline intrusion, South Greenland. Bulletin Grønlands Geologiske Undersøgelse 39, 82pp.

Flesch G.D., Anderson A.R. and Svec H.J. (1973)
A secondary isotopic standard for $^{6}Li/^{7}Li$ determinations. International Journal of Mass Spectrometry and Ion Processes, 12, 265-272.

Halama R., McDonough W.F., Rudnick R.L., Keller J. and Klaudius J. (2007)
The Li isotopic composition of Oldoinyo Lengai: Nature of the mantle sources and lack of isotopic fractionation during carbonatite genesis. Earth and Planetary Science Letters, 254, 77-89.

Hauri E.H., Shaw A.M., Wang, J., Dixon J.E., King P.L. and Mandeville C. (2006)
Matrix effects in hydrogen isotope analysis of silicate glasses by SIMS. Chemical Geology, 235, 352-365.

Jeffcoate A., Elliott T., Kasemann S.A., Ionov D.A., Cooper K.M. and Brooker R.A. (2007)
Li isotope fractionation in peridotites and mafic melts. Geochimica et Cosmochimica Acta, 71, 202-218.

Jochum K.P., Willbold M., Raczek I., Stoll B. and Herwig K. (2005)
Chemical characterisation of the USGS reference glasses GSA-1G, GSC-1G, GSD-1G, GSE-1G, BCR-2G, BHVO-2G and BIR-1G using EPMA, ID-TIMS, ID-ICP-MS and LA-ICP-MS. Geostandards and Geoanalytical Research, 29, 285-302.

Kasemann S.A., Jeffcoate A. and Elliott T. (2005)
Lithium isotope composition of basalt glass reference material. Analytical Chemistry, 77, 5251-5257.

Krumrei T.V., Villa I.M., Marks M.A.W. and Markl G. (2006)
A $^{40}Ar/^{39}Ar$ and U/Pb isotopic study of the Ilimaussaq complex, South Greenland: Implications for the ^{40}K decay constant and for the duration of magmatic activity in a peralkaline complex. Chemical Geology, 227, 258-273.

Larsen L.M. (1976)
Clinopyroxenes and coexisting mafic minerals from the alkaline Ilimaussaq intrusion, south Greenland. Journal of Petrology, 17, 258-290.

Larsen L.M. (1981)
Sector zoned aegirine from the Ilimaussaq alkaline intrusion, South Greenland. Contributions to Mineralogy and Petrology, 76, 285-291.

Leake B.E., Wooley A.R., Arps C.E.S., Birch W.D., Gilbert M.C., Grice J.D., Hawthorne F.C., Kato A., Kisch H.J., Krivovichev V.G., Linthout K., Laird J., Mandarino J.A., Maresch W.V., Nickel E.H., Rock N.M.S., Schumacher J.C., Smith D.C., Stephenson N.C.N., Ungaretti L., Whittaker E.J.W. and Youzhi G. (1997)
Nomenclature of amphiboles: Report of the subcommittee on amphiboles of the International Mineralogical Association, Commission on new minerals and mineral names. American Mineralogist, 82, 1019-1037.

Lundstrom C.C., Chaussidon M., Hsui A.T., Kelemen P.B. and Zimmermann M. (2005)
Observations of Li isotopic variations in the Trinity Ophiolite: Evidence for isotopic fractionation by diffusion during mantle melting. Geochimica et Cosmochimica Acta, 69, 735-751.

Ludwig T., Marschall H.M. and Altherr R. (2004)
Is there a matrix effect in SIMS boron isotope analysis? Geochimica et Cosmochimica Acta, 68, Supplement 1, A54.

Markl G., Marks M., Schwinn G. and Sommer H. (2001)
Phase equilibrium constraints on intensive crystallization parameters of the Ilimaussaq Complex, South Greenland. Journal of Petrology, 42, 2231-2258.

Marks M.A.W., Vennemann T., Siebel W. and Markl G. (2004)
Nd-, O-, and H-isotopic evidence for complex, closed-system fluid evolution of the peralkaline Ilimaussaq Intrusion, South Greenland. Geochimica et Cosmochimica Acta, 68, 3379-3395.

Marks M.A.W., Rudnick R.L., McCammon C., Vennemann T. and Markl G. (2007)
Arrested kinetic Li isotope fractionation at the margin of the Ilímaussaq complex: Evidence for open-system processes during final cooling of peralkaline igneous rocks. Chemical Geology, 246, 207-230.

Marschall H.R., Altherr R., Ludwig T., Kalt A., Gméling K. and Kasztovsky Z. (2006)
Partitioning and budget of Li, Be and B in high-pressure metamorphic rocks. Geochimica et Cosmochimica Acta, 70, 4750-4769.

Marschall H.R. and Ludwig T. (2004)
The low-boron contest: Minimising surface contamination and analysing boron concentrations at the ng/g-level by secondary ion mass spectrometry. Mineralogy and Petrology, 81, 265-278.

Morimoto N., Fabries J., Ferguson A.K., Ginzburg I.V., Ross M., Seifeit F.A. and Zussmann J. (1989)
Nomenclature of pyroxenes. The Canadian Mineralogist, 27, 143-156.

Müller-Lorch D., Marks M.A.W. and Markl G. (2007)
Na and K distribution in agpaitic pegmatites. Lithos, 95, 315-330.

references

Ottolini L., Le Fèvre B. and Vanucci R. (2004)
Direct assessment of mantle boron and lithium contents and distribution by SIMS analyses of peridotite minerals. Earth and Planetary Science Letters, 228, 19-36.

Ottolini L., Bottazzi P. and Vanucci R. (1993)
Quantification of lithium, beryllium, and boron in silicates by secondary ion mass spectrometry using conventional energy filtering. Analytical Chemistry, 65, 1961-1968.

Parkinson I.J., Hammond S.J., James R.H. and Rogers N.W. (2007)
High-temperature lithium isotope fractionation: Insights from lithium isotope diffusion in magmatic systems. Earth and Planetary Science Letters 257, 609-621.

Pearce N.J.G., Perkins W.T., Westgate J.A., Gorton M.P., Jackson S.E., Neal C.R. and Chenery S.P. (1997)
A compilation of new and published major and trace element data for NIST SRM 610 and NIST SRM 612 glass reference materials. Geostandards Newsletter: The Journal of Geostandards and Geoanalysis, 21, 115-144.

Richter F.M., Davis A.M., DePaolo D. and Watson E.B. (2003)
Isotope fractionation by chemical diffusion between molten basalt and rhyolite. Geochimica et Cosmochimica Acta, 67, 3905-3923.

Rosner M., Wiedenbeck M. and Ludwig T. (2008)
Composition-induced variations in SIMS instrumental mass fractionation during boron isotope ratio measurements of silicate glasses. Geostandards and Geoanalytical Research, 32, 27-38.

Rudnick R. and Ionov D.A. (2007)
Lithium elemental and isotopic disequilibrium in minerals from peridotite xenoliths from far-east Russia: Product of recent melt/fluid-rock reaction. Earth and Planetary Science Letters, 256, 278-293.

Rudnick R. and Nakamura E. (2004)
Preface to "Lithium isotope geochemistry". Chemical Geology, 212, 1-4.

Rudnick R., Tomascak P.B., Njo H.B. and Gardner L.R. (2004)
Extreme lithium isotopic fractionation during continental weathering revealed in saprolites from South Carolina. Chemical Geology, 212, 45-57.

Ryan J.G. and Langmuir C.H. (1987)
The systematics of lithium abundances in young volcanic rocks. Geochimica et Cosmochimica Acta, 51, 1727-1741.

Seitz H.-M., Brey G.P., Lahaye Y., Durali S. and Weyer S. (2004)
Lithium isotopic signatures of peridotite xenoliths and isotopic fractionation at high temperature between olivine and pyroxenes. Chemical Geology, 212, 163-177.

Sørensen H. (1997)
The agpaitic rocks - an overview. Mineralogical Magazine, 61, 485-498.

Sørensen H. (2001)
Brief introduction to the geology of the Ilimaussaq alkaline complex, South Greenland. Geology of Greenland Survey Bulletin, 190, 7-24.

Sørensen H. (2006)
The Ilímaussaq alkaline complex, South Greenland - an overview of 200 years of research and an outlook. Meddelelser om Grønland, 45, 70pp.

Teng F.-Z., McDonough W.F., Rudnick R., Dalpé C., Tomascak P.B., Chappell B.W. and Gao S. (2004)
Lithium isotopic composition and concentration of the upper continental crust. Geochimica et Cosmochimica Acta, 68, 4167-4178.

Teng F.-Z., McDonough W.F., Rudnick R., Walker R.J. and Sirbescu M.-L.C. (2006)
Lithium isotopic systematics of granites and pegmatites from Black Hills, South Dakota. American Mineralogist, 91, 1488-1498.

Tischendorf G., Förster H.-J. and Gottesmann B. (2001)
Minor- and trace-element composition of trioctahedral micas: A review. Mineralogical Magazine, 65, 249-276.

Tomascak P.B. (2004)
Developments in the understanding and application of Lithium isotopes in the Earth and planetary sciences. Reviews in Mineralogy and Geochemistry, 55, 153-195.

Tomascak P.B., Carlson R.W. and Shirey S.B. (1999)
Accurate and precise determination of Li isotopic compositions by multi-collector ICP-MS. Chemical Geology, 158, 145-154.

Williams L.B. and Hervig R.L. (2005)
Lithium and boron isotopes in illite-smectite: The importance of crystal size. Geochimica et Cosmochimica Acta, 69, 5705-5716.

Zack T., Tomascak P.B., Rudnick R.L., Dalpé C. and McDonough W.F. (2003)
Extremely light Li in orogenic eclogites: The role of isotope fractionation during dehydration in subducted oceanic crust. Earth and Planetary Science Letters, 208, 279-290.